

Twist1 regulates embryonic hematopoietic differentiation through binding to *Myb* and *Gata2* promoter regions

Kasem Kulkeaw,^{1,*} Tomoko Inoue,^{1,*} Tadafumi Iino,² Kenzaburo Tani,³ Koichi Akashi,^{2,4} Nancy A. Speck,⁵ Yoichi Nakanishi,⁶ and Daisuke Sugiyama^{1,6,7}

¹Department of Research and Development of Next Generation Medicine, Faculty of Medical Sciences, Kyushu University, Fukuoka, Japan; ²Center for Cellular and Molecular Medicine, Kyushu University Hospital, Fukuoka, Japan; ³Project Division of ALA Advanced Medical Research, The Institute of Medical Science, The University of Tokyo, Tokyo, Japan; ⁴Department of Medicine and Biosystemic Science, Kyushu University Graduate School of Medical Sciences, Fukuoka, Japan; ⁵Abramson Family Cancer Research Institute, Department of Cell and Developmental Biology, Perelman School of Medicine, University of Pennsylvania, Philadelphia, PA; ⁶Center for Clinical and Translational Research, Kyushu University Hospital, Fukuoka, Japan; and ⁷Department of Clinical Study, Center for Advanced Medical Innovation, Kyushu University, Fukuoka, Japan

Key Points

- Twist1, a hematopoietic transcription factor, is highly expressed in embryonic HSPCs.
- Twist1 functions in embryonic HSPC differentiation through binding to *Myb* and *Gata2* promoter regions and activates their transcription.

Mechanisms underlying differentiation of embryonic hematopoietic stem/progenitor cells (HSPCs) remain unclear. In mouse, intra-aortic clusters (IACs) form in the aorta-gonad-mesonephros region and acquire HSPC potential after 9.5 days postcoitum (dpc). In this study we demonstrate that Twist1 is highly expressed in c-Kit⁺CD31⁺CD34⁺ IACs, which are equivalent to embryonic HSPCs, compared with adult HSPCs. Progenitor activities of colony-forming unit (CFU) of granulocytes and macrophages, CFU of macrophages, burst-forming unit of erythroid, and B lymphopoiesis were impaired in IACs of *Twist1*^{-/-} relative to wild-type embryos. Microarray analysis and real-time polymerase chain reaction showed downregulated expression of *Myb* and *Gata2* transcripts in *Twist1*^{-/-} IACs. Chromatin immunoprecipitation and promoter binding assays indicated that Twist1 directly binds the *Myb* and *Gata2* promoters in 10.5-dpc IACs. We conclude that Twist1 is a novel transcriptional regulator of HSPC differentiation through direct binding to promoter regions of key regulators of the process.

Introduction

Hematopoiesis occurs in distinct hematopoietic organs throughout embryogenesis. In the mouse embryo, hematopoietic stem cells with the ability to differentiate into all types of hematopoietic cells, and hematopoietic progenitor cells with restricted hematopoietic potential relative to hematopoietic stem cells, are detected in the para-aortic-splanchnopleural (p-Sp)/aorta-gonad-mesonephros (AGM) region, the placenta, and, to a lesser extent, the yolk sac.¹⁻⁶ Hematopoietic stem/progenitor cells (HSPCs) then colonize fetal liver, where they expand and differentiate into mature hematopoietic cells. Thus, the AGM region is an important site of definitive hematopoietic activity. Intra-aortic clusters (IACs) form in the AGM and in the floors of large arteries, such as the dorsal aorta (DA),⁷ the omphalomesenteric (vitelline) artery (OA), and the umbilical artery (UA),^{3,8,9} as if IACs emerge from endothelium of these arteries.

That IACs acquire HSPC potential is based on evidence derived from hematopoietic transplantation assays, and HSPCs are characterized as cells expressing c-Kit, CD31, and CD34.¹⁰ In mice, from 9.5 to 11.5 days postcoitum (dpc), expression of CD45, a pan-leukocyte marker, is upregulated in the IAC population.^{7,10} In addition, the appearance of a nascent HSPC marker, CD41, marks emergence of HSPCs from endothelial cells lining the DA.⁵ Generation of IACs is intrinsically regulated by transcription factors such as Runx1,^{11,12} *Myb*,¹³ *Gata2*,¹⁴ *Scf/Tal1*,¹⁵ and *Mecom* (*Evi-1*).^{16,17} A transcription switch

reportedly occurs at 9.5 to 10.5 dpc, based on cap analysis of gene expression.¹⁸ By contrast, IAC differentiation is extrinsically regulated by the AGM region niche. The mesonephros, a component of that region, is localized underneath IACs, and CSF1 secretion from mesonephros accelerates myeloid differentiation.¹⁹ However, mechanisms regulating HSPC differentiation in early embryogenesis remain unclear.

Twist1 is a class II basic helix-loop-helix domain-containing protein that functions as a transcriptional regulator of osteoblast²⁰ and mesenchymal cell differentiation.^{21,22} *Twist1*^{-/-} mice exhibit craniofacial defects at 10.5 dpc^{23,24} and die at 11.5 dpc because of vascular and cranial neural tube defects.²⁵ We previously generated a data set of HSPC transcripts by cap analysis during ontogeny and found that *Twist1* is more highly expressed in embryonic relative to adult HSPCs.¹⁸

Here, for the first time, we use a gene knockout approach to demonstrate that Twist1 functions in IAC hematopoietic differentiation in embryonic mouse. Specifically, we show impaired hematopoietic differentiation of IAC in colony formation assay and transcriptional activity of Twist1 in *Myb* and *Gata2* promoter regions of IAC. These observations strongly suggest overall that Twist1 regulates HSPC differentiation through binding to *Myb* and *Gata2* promoter regions.

Methods

Mice

C57BL/6 mice (SLC, Hamamatsu, Japan) and heterozygous *Twist1* mutant (*Twist1*^{tm1Bhr}/*Twist1*⁺ or *Twist1*^{+/-}) mice used in this study were purchased from the Jackson Laboratory. Noon of the day of the plug was considered 0.5 dpc. Embryos at 9.5, 10.5, and 14.5 dpc were dissected in phosphate-buffered saline (PBS) under a stereomicroscope, and the number of somite pairs was counted.²⁶ Animals were handled according to Guidelines for Laboratory Animals of Kyushu University. This study was approved by the Animal Care and Use Committee, Kyushu University (Approval ID: A21-068-0).

Immunohistochemistry

Embryos at 10.5 dpc were dissected and fixed in 2% paraformaldehyde in PBS at 4°C overnight, followed by equilibration with 30% sucrose in PBS. Embryos were embedded in optimal cutting temperature compound (Sakura, Tokyo, Japan) and frozen in liquid nitrogen. Tissues were sliced at 20 μm using a Leica CM1900 UV cryostat (Leica Microsystems, Tokyo, Japan), transferred to glass slides (Matsunami Glass, Osaka, Japan), and dried. Sections were blocked with 1% bovine serum albumin in PBS and incubated overnight at 4°C with indicated dilutions of the following primary antibodies: rabbit anti-mouse Twist1 (1:50, sc-15393; Santa Cruz Biotechnology, Santa Cruz, CA), rat anti-mouse CD31 (1:300, MEC13.3; BD Biosciences, San Diego, CA), and rat anti-mouse CD34 (1:300, RAM34; eBioscience, San Diego, CA). After 3 PBS washes, sections were incubated 30 minutes at room temperature with appropriate dilutions of Alexa Fluor 488 goat anti-rabbit IgG (1:400; Life Technologies, Gaithersburg, MD) and Alexa Fluor 549 goat anti-rat IgG (1:400; Life Technologies) secondary antibodies, as well as TOTO-3 (1:3000; Life Technologies). Sections were washed 3 times with PBS, mounted on coverslips with fluorescence mounting medium (Dako Corporation, Carpinteria,

CA), and assessed using a Fluo View 1000 confocal microscope (Olympus, Tokyo, Japan).

Cell preparation

A single cell suspension was obtained from the caudal portion of 9.5- and 10.5-dpc embryos containing the p-Sp/AGM region, as described.¹⁰ Briefly, tissues were incubated 30 minutes with 1 mg/mL collagenase in α-minimum essential medium supplemented with 10% fetal bovine serum (FBS) at 37°C and filtered through 40-μm nylon cell strainers (BD Biosciences). Fetal liver (FL) and bone marrow (BM) hematopoietic cells were prepared as described.¹⁸ Briefly, FL was dissected from 14.5-dpc embryos, and FL hematopoietic cells were prepared by mashing FL on a 40-μm nylon cell strainer (BD Biosciences). BM cells from femurs and tibias of 2- to 3-month-old mice were dissected and flushed with PBS containing 2% FBS using 27G needles and syringes (Terumo, Tokyo, Japan). Cells then were filtered through 40-μm nylon cell strainers and washed with 2% FBS in PBS.

Flow cytometric analysis and cell sorting

Antibodies used for analysis of 9.5-dpc p-Sp/AGM region were fluorescein isothiocyanate (FITC)-conjugated anti-mouse CD31 (BD Biosciences), phycoerythrin (PE)-conjugated anti-mouse CD34 (eBioscience), and allophycocyanin (APC)-conjugated anti-mouse c-Kit (Biolegend, San Diego, CA). FITC-conjugated anti-mouse CD34 (eBioscience), PE-conjugated anti-mouse CD31 (Biolegend), and APC-conjugated anti-mouse c-Kit were used for analysis of AGM at 10.5 dpc. FITC-conjugated anti-mouse CD45 (BD Bioscience); PE-conjugated anti-mouse Sca1 (BD Bioscience); APC-conjugated anti-mouse c-Kit; biotin-conjugated anti-mouse Ter119, Gr-1, B220, CD4, CD8 (all from Biolegend); and PB-conjugated streptavidin (eBioscience) were used for analysis of 14.5-dpc FL and 2- to 3-month-old mice. Cells were sorted with BD FACS Aria (BD Bioscience). Data files were analyzed using FlowJo software (Tree Star Inc., San Carlos, CA).

Colony-forming unit (CFU) assay

Bulk cells of AGM were suspended in 3 mL MethoCult GF M3434 methylcellulose medium (StemCell Technologies Inc., Vancouver, BC, Canada) and split into 3 35-mm dishes. Preparations were then cultured in 5% CO₂ at 37°C. Resulting colonies were characterized on day 9 using an inverted phase contrast microscope CKX41 (Olympus, Tokyo, Japan).

In vitro B lymphopoiesis assay

B lymphoid differentiation was assessed as reported.²⁷ Single cells were prepared from AGM and cocultured with OP9 stromal cells in α-minimum essential medium supplemented with 10% fetal calf serum (Hyclone Laboratory, Logan, UT), 5 × 10⁻⁵ M 2-mercaptoethanol (Eastman Organic Chemicals, Rochester, NY), 50 ng/mL mouse stem cell factor (SCF) and 200 U/mL mouse interleukin-7 (IL-7). At days 12 to 14 of culture, cells were analyzed for CD19 and B220 by flow cytometry. Replicate wells were set up for analysis of wild-type (WT), *Twist1*^{+/-}, and *Twist1*^{-/-} AGM.

RNA extraction and real-time polymerase chain reaction (PCR)

Total RNA was isolated from sorted cells and treated with DNase I using an RNAqueous-4PCR Kit and RNAqueous-Micro Kit (Ambion

Table 1. Sequences of primers used in this study

Purpose	Forward primer (5'–3')	Reverse primer (5'–3')
ChIP-quantitative PCR		
<i>Myb</i> promoter	CTCCCGGTGTGTTGAAGTC	GCTCCCGAGCCCGAAT
<i>Gata2</i> promoter	CTACCAGCCTCTTGACACAGCTA	GCCCCACCTCCACTGCTA
Luciferase activity		
<i>Myb</i> promoter	CTCCCGGTACCGTTGAAGTCGGGGCGCAGTT	GTGTACCCCAACCCATCGAGAGCTCCTTGAA
Mutant <i>Myb</i> promoter	GTTGAAGTCGGGGCGATGTAGAACCCTGA AGG	CCTTCAGGGTTTCTACATCGCCCCGACTTCAAC
<i>Gata2</i> promoter	GATAGAGGTACCGAGAGTTTGGGGAGTCAGTT	CCGTAGCAGTGGAGGTGGGGGAGCTCCTCCGC
Mutant <i>Gata2</i> promoter	GAGAGTTTGGGGAGTATGTAGGATTTGGGCTGG	CCAGCCCAATCTACATACTCCCAAACTCTC
Endothelial-specific genes		
<i>Cdh5</i>	ACCGCTGATCGGCACTGT	TCGGAAGAATTGGCCTCTGT
<i>Tek</i>	GATACAGCCTTTCCATCCTAATCT	CAGAAGCAGGCGGTAACAGTCT

Inc., Austin, TX), according to the manufacturer's instructions. Total RNA was subjected to reverse transcription using a High-Capacity RNA-to-cDNA Kit (Life Technologies, Carlsbad, CA) according to the manufacturer's instructions. Transcript levels were measured by real-time PCR (StepOnePlus real time PCR; Life Technologies) using TaqMan Gene Expression Master Mix (Life Technologies). *Twist1* (Mm00442036_m1), *Myb* (Mm00501741_m1), *Gata2* (Mm00492301_m1), *Runx1* (Mm00516096_m1), *Mecom* (Mm00514814_m1), *Gata1* (Mm01352636_m1), *Klf1* (Mm00516096_m1), *Spi1* (*Pu.1* Mm00488142_m1), and *Csf1r* (Mm01266652_m1) probes were from TaqMan Gene Expression Assays (Life Technologies). Amplification conditions were as follows: initial denaturation at 95°C for 10 seconds, annealing at 60°C for 20 seconds (30 cycles), and extension at 72°C for 20 seconds. A final dissociation step was 95°C for 15 seconds, 60°C for 1 minute, and 95°C for 15 seconds. *Actb* (Mm00607939_m1) served as internal control to normalize gene expression. Gene expression was compared with a reference sample using the $2^{-\Delta\Delta CT}$ method²⁸ and is shown as comparative expression. Experiments were carried out in triplicate.

Chromatin immunoprecipitation (ChIP) assay

Cross-linking was performed by adding a 37% formaldehyde solution (Wako Pure Chemical Industries, Osaka, Japan) to a final concentration of 1% to sorted c-Kit⁺CD31⁺CD34⁺ cells of mouse 10.5-dpc AGM. Cross-linking proceeded at room temperature for 10 minutes, and cells were lysed in sodium dodecyl sulfate lysis buffer containing protease inhibitors. Chromatin was sonicated to 400 to 800 bp fragments. Immunoprecipitation was performed using a Chromatin Immunoprecipitation Assay Kit (Millipore, MA), according to the manufacturer's instructions. Immunoprecipitation was carried out overnight with rabbit polyclonal Twist H-81 antibody (2 μg; Santa Cruz Biotechnology) or rabbit isotype antibody at 4°C. Immune complexes were precipitated, washed, and eluted. After precipitation, supernatants were processed for the cross-link reversal step. Nonimmunoprecipitated samples served as input chromatin. After proteinase K digestion, samples were phenol extracted, and genomic DNA was ethanol precipitated and resuspended in 10 μL H₂O. The amount of *Myb* and *Gata2*

promoter in total input and immunoprecipitated DNA was measured using real-time PCR (StepOnePlus real time PCR; Life Technologies) with primer sets and Fast SYBR Green Master Mix (AB Applied Biosystems, CA). Primer sets bound to the promoter region located between 500 bp at 5'-end and 100 bp at 3'-end from the transcriptional start site, as predicted using the DataBase of Transcriptional Start Sites²⁹ (<http://dbtss.hgc.jp/>). Primer sets were designed using Primer Express version 3.0 (Table 1). Thermal cycle conditions were as follows: 1 cycle of denaturation at 95°C for 20 seconds and 40 cycles of denaturation at 95°C for 3 seconds, and annealing and extension at 60°C for 30 seconds. A final dissociation step consisted of 95°C for 15 seconds, 60°C for 1 minute, and 95°C for 15 seconds.

Luciferase reporter assays

A Twist1-binding hexanucleotide sequence (CANNTG; E-box) was identified and located 5' of predicted *Myb* or *Gata2* transcriptional start sites, which were predicted as indicated previously. A 58-bp PCR product containing the sequence was amplified from mouse tail genomic DNA and subcloned into a firefly luciferase reporter plasmid pGL4.10[luc2]. For some constructs, a loss-of-function mutation was introduced into the hexanucleotide based on the manufacturer's instructions (QuikChange Site-Directed Mutagenesis kit; Agilent Technologies, Santa Clara, CA). Primers are shown in Table 1. The Twist1 expression plasmid pCMV6-Entry was obtained from Origene. Luciferase plasmids (pGL4.10[luc2]-*Myb* promoter and pGL4.10[luc2]-*Gata2* promoter), Twist1 expression plasmids (pCMV6-Entry-Twist1), and a *Renilla* luciferase reference gene (pGL4.74 hRluc/TK) plasmid as an internal control were cotransfected into 293Ta cells with Lipofectamine 2000 (Thermo Fisher Scientific). After 66 hours, cells were harvested using passive lysis buffer (Promega, Madison, WI). Cell lysates were evaluated for luciferase activity using the Dual-Luciferase reporter assay kit (Promega). Luciferase activity was measured according to the manufacturer's instructions and normalized to *Renilla* luciferase values. Promoter activity (firefly/*Renilla* luciferase) is represented as fold induction relative to luciferase activity obtained from mutant *Myb* and *Gata2* promoter-containing pGL4.10[luc2] constructs. Triplicate wells were evaluated.

Statistical analysis

Data are presented as means \pm standard deviation (SD). Differences were statistically evaluated using Student *t* test. *P* values $<.05$ were considered statistically significant.

Results

Twist1 is expressed in mouse embryo IACs

To examine spatiotemporal expression of *Twist1* in mouse hematopoietic cells, we compared levels of *Twist1* transcripts in (1) c-Kit⁺CD31⁺CD34⁺ cells recognized as IACs in 9.5-dpc and 10.5-dpc AGM regions, (2) Lineage⁻c-Kit⁺Sca1⁺CD45⁺ cells recognized as HSPCs in 14.5-dpc FL, and (3) Lineage⁻c-Kit⁺Sca1⁺ as HSPCs in 2- to 3-month-old BM by real-time PCR (Figure 1A-B). *Twist1* transcript levels in 10.5-dpc AGM-derived IACs decreased 1.25-fold relative to those seen in 9.5-dpc IACs (Figure 1B; *P* $<.05$). *Twist1* transcript levels in 14.5-dpc FL-derived HSPCs decreased 124- and 99.3-fold compared with those in respective 9.5-dpc and 10.5-dpc AGM-derived IACs (Figure 1B; *P* $<.05$). *Twist1* transcript levels in BM-derived Lineage⁻c-Kit⁺Sca1⁺ HSPCs were similar to those seen in 14.5-dpc FL-derived HSPCs. *Twist1* transcript levels in BM-derived Lineage⁻c-Kit⁺Sca1⁺ HSPCs decreased 82.4- and 66-fold compared with levels in respective 9.5-dpc and 10.5-dpc AGM-derived IACs (Figure 1B; *P* $<.05$).

Next, we confirmed Twist1 protein expression by performing immunohistochemistry of AGM regions at 10.5 dpc. To assess quality of the anti-Twist1 antibody, we immunostained sorted 10.5-dpc AGM IACs and 2- to 3-month-old BM Lineage⁻c-Kit⁺Sca1⁺ HSPCs. Twist1 protein was observed in the nucleus and cytoplasm of AGM-derived IACs and BM-derived HSPCs. Based on fluorescence intensity, Twist1 protein levels paralleled levels of *Twist1* transcripts (supplemental Figure 1), suggesting that the antibody efficiently detects Twist1 protein.

Aggregates of >3 CD31⁺ or CD34⁺ cells were defined as IACs.^{10,19} IACs expressing CD31 (Figure 1C, left panel) or CD34 (Figure 1C, right panel) were observed in the DA at 10.5 dpc. Twist1 protein was seen in the cytoplasm and nucleus of IACs expressing CD31 (Figure 1C, left panel in dashed box) or CD34 (Figure 1C, right panel in dashed box). DA endothelial cells also expressed Twist1 protein (Figure 1C, arrowhead in right panel of dashed box). Taken together, *Twist1* messenger RNA and protein are expressed in IACs at 9.5 to 10.5 dpc.

Twist1^{-/-} IACs show impaired hematopoietic differentiation ability

To investigate Twist1 function in hematopoietic development and IAC differentiation, we employed *Twist1* knockout mice. Compared with WT embryos, *Twist1*^{-/-} embryos exhibit smaller body and head (Figure 2A). IACs were observed in the 10.5-dpc WT DA, OA, and UA.¹⁰ We observed IACs only in the OA, and not the DA or UA, of *Twist1*^{-/-} embryos at 10.5 dpc (Figure 2B, arrows). Flow cytometric analysis showed that c-Kit⁺CD31⁺CD34⁺ IACs comprised 1.44% \pm 0.53 of all cells in the AGM region of WT embryos, 0.99% \pm 0.37 in the AGM of *Twist1*^{+/-} embryos, and 1.89% \pm 0.94 in the AGM of *Twist1*^{-/-} embryos, differences that were not statistically significant (Figure 2C; supplemental Figure 2).

Next, we examined Twist1 function in IAC differentiation. We prepared single cells from AGM of 10.5-dpc WT, *Twist1*^{+/-}, and

Twist1^{-/-} embryos and plated them for a CFU assay. In the presence of the erythro-myeloid lineage-promoting cytokines SCF, IL-3, IL-6, and erythropoietin, total colony numbers per AGM region decreased by 1.6-fold (*P* = .209) in heterozygotes compared with WT embryos, and those of homozygotes decreased by 5.4-fold (*P* = .007) (Figure 2D). Regarding lineage types of hematopoietic colonies (Figure 2E), there was no difference in numbers of CFU-GEMM (*P* = .76), CFU-GM (*P* = .14), CFU-M (*P* = .93), CFU-G (*P* = .30), and BFU-E (*P* = .17) in heterozygous vs WT AGM regions, whereas the AGM region of *Twist1* homozygotes showed a 4.66-fold decrease in the number of CFU-GEMM (*P* = .18), a 7.97-fold decrease in CFU-GM (*P* = .004), a 2.89-fold decrease in CFU-M (*P* = .003), and a 4.49-fold decrease in BFU-E colonies (*P* = .031) relative to WT (Figure 2E; supplemental Figure 3A). No CFU-G was observed in cells derived from the *Twist1*^{-/-} AGM region. Moreover, relative to WT embryos, B lymphoid differentiation ability of 10.5-dpc *Twist1*^{-/-} embryos decreased in OP9 cell coculture analysis (Figure 2F). In agreement with the CFU assay, levels of transcripts encoding the erythroid transcription factors Gata1 and Klf1, but not the myeloid transcription factor Spi1 factor and its target Csf1r, decreased in *Twist1*^{-/-} IACs relative to levels seen in WT IACs (Figure 2G).

Next, we evaluated differentiation of *Twist1* knockout HSPCs migrating from 10.5-dpc AGM to 11.5-dpc FL. Given that *Twist1*^{-/-} embryos die at 11.5-dpc,²⁵ to perform this analysis we prepared single cells from FL of 11.5-dpc *Twist1*^{+/-} embryos and performed a CFU assay. We observed no difference in the percentage of FL HSPCs, defined as Lineage⁻Sca1⁺c-Kit⁺CD45⁺ cells, in 11.5-dpc WT (*n* = 4) and *Twist1*^{+/-} (*n* = 3) embryos (*P* = .87). Total colony numbers per FL of 11.5-dpc *Twist1*^{+/-} (*n* = 3) embryos were similar to numbers derived from WT embryos (*n* = 3) (*P* = .41). We observed no difference in the number of CFU-GEMM (*P* = .68), CFU-GM (*P* = .45), CFU-M (*P* = .74), CFU-G (*P* = .79), and BFU-E (*P* = .57) in heterozygous vs WT FL samples (supplemental Figure 3C). Moreover, in terms of hematopoiesis, we observed no difference in peripheral blood parameters in adult *Twist1*^{+/-} vs WT mice (supplemental Figure 4). Overall, we conclude that IAC hematopoietic differentiation ability is impaired in AGM of *Twist1*^{-/-} embryos.

IACs from the Twist1^{-/-} AGM region show downregulation of genes encoding hematopoietic transcription factors

We next investigated mechanisms underlying impaired hematopoietic differentiation capacity of *Twist1*^{-/-} IACs. Given that Twist1 functions as a transcription regulator, we examined global gene expression in 10.5-dpc WT and *Twist1*^{+/-} IACs, defined as c-Kit⁺CD31⁺CD34⁺ cells, by microarray (supplemental Table 1). Because of the limited number of *Twist1*^{-/-} IACs, we examined only gene expression in *Twist1*^{+/-} IACs. Specification of endothelial cells to a definitive hematopoietic fate occurs in the AGM region, a process called the endothelial-to-hematopoietic (ETH) transition. To determine whether hematopoietic fate of AGM-derived IACs is fully specified in *Twist1* knockout embryos, we analyzed potential transcriptional changes in expression of the endothelial genes *Cdh5*, *Tek*, *Esam*, *Kdr*, *Eng*, and *Gpr56*^{30,31} by microarray data. *Cdh5* and *Tek* transcripts were upregulated in *Twist1*^{+/-} IACs compared with WT samples (supplemental Figure 5A). We observed no *Esam*, *Kdr*, *Eng* and *Gpr56* signals in IACs of WT

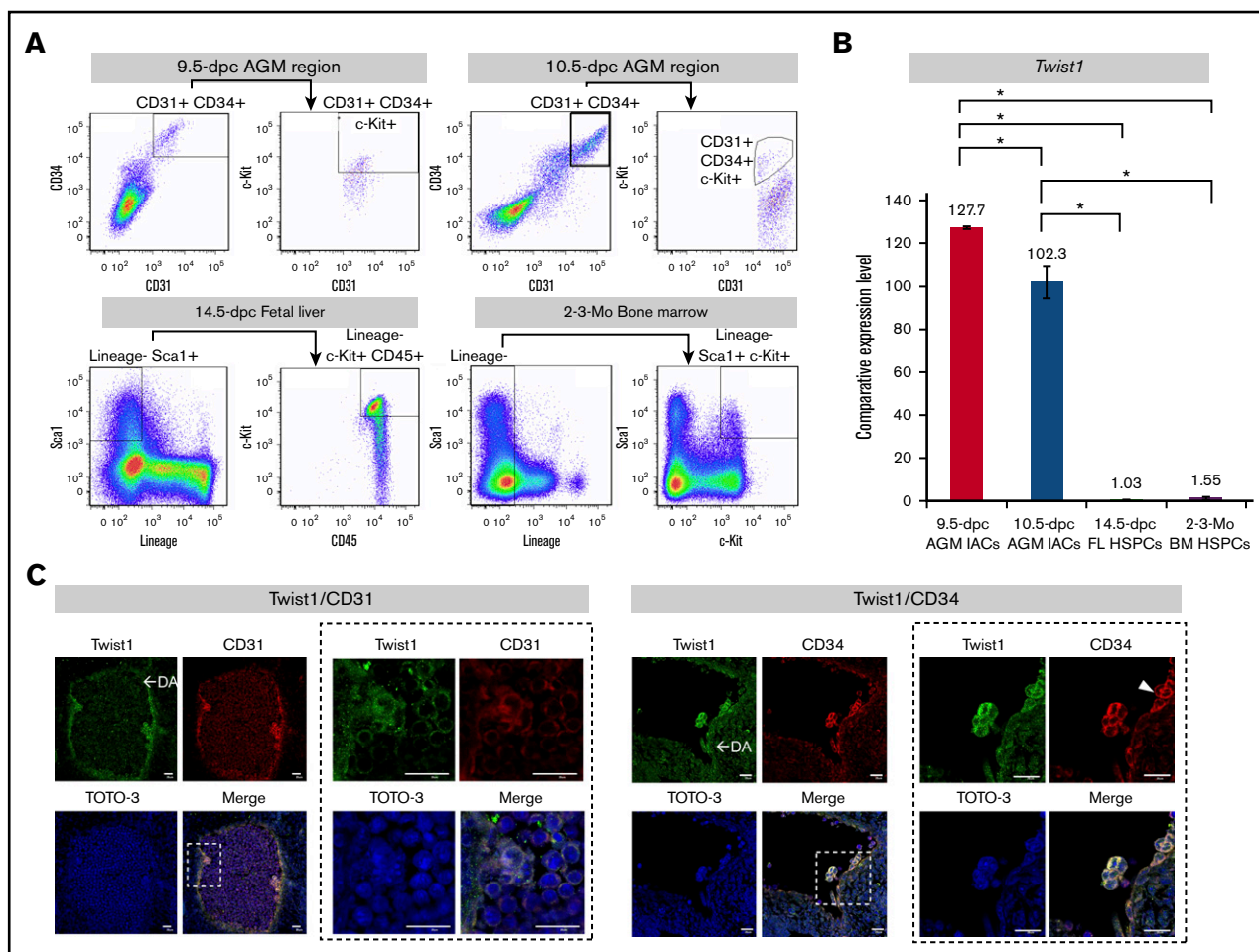


Figure 1. IACs express *Twist1* at midgestation in mice. (A) Flow cytometric analysis of HSPCs over the course of development. Single cell suspensions of the caudal portion of embryos containing the p-Sp/AGM region at 9.5 dpc (upper left) and 10.5 dpc (upper right) were prepared. Cells expressing both CD31 and CD34 were gated first, and then among those cells, c-Kit⁺ cells were analyzed. FL cells at 14.5 dpc (lower left) were also prepared. Lineage⁻ Sca1⁺ cells were gated first, and then among them, c-Kit⁺ and CD45⁺ cells were analyzed. BM cells at 2 to 3 months old (lower right) were prepared. Lineage⁻ cells were gated, and c-Kit⁺ and Sca1⁺ cells were analyzed among Lineage⁻ cells. Images are representative of 3 independent flow cytometric analyses (n = 3). (B) *Twist1* expression in HSPCs. RNA was extracted from sorted HSPCs at 9.5-dpc and 10.5-dpc AGM region, 14.5-dpc FL, and 2- to 3-month-old BM shown in panel A, and *Twist* expression assessed using a TaqMan probe. Comparative expression levels were calculated using the 2^{- $\Delta\Delta$ CT} method. The 14.5-dpc FL HSPC sample served as a reference. Data shown are means \pm SD of technical triplicate samples. **P* < .05. (C) Confocal images of IACs expressing *Twist1*, CD31, and CD34 in AGM. AGM region sections were prepared from C57BL/6 mouse embryos at 10.5 dpc, stained with indicated antibodies, and observed by confocal microscopy. Left panels show *Twist1* (green), CD31 (red), and TOTO-3 (blue) staining. Right panels show *Twist1* (green), CD34 (red), and TOTO-3 (blue) staining. Magnified views of respective dashed boxes are shown adjacent at right. Bars represent 20 μ m for all panels.

and *Twist1*^{+/-} samples. We next assessed *Cdh5* and *Tek* expression in IACs by real-time PCR and found that levels of both increased by 1.4-fold (*P* = .02) and 1.6-fold (*P* = .01), respectively, in *Twist1* homozygotes relative to WT cells (supplemental Figure 5B). We observed no differences in *Cdh5* and *Tek* transcript levels in WT and *Twist1*^{+/-} IACs.

Next we focused on representative hematopoietic transcription factor genes, namely, *Myb*,^{13,32} *Gata2*,¹⁴ *Runx1*,¹² *Tal1* (*Scf*),¹⁵ and *Mecom* (*Evi-1*),^{16,17} as these factors play important roles in HSPC generation and differentiation. Among them, levels of *Myb*, *Gata2*, and *Mecom* were higher than those of *Runx1* and *Tal1* in microarrays of c-Kit⁺CD31⁺CD34⁺ cells derived from AGM of 10.5-dpc WT embryos (Figure 3A, white bars). Compared with WT embryos, expression levels of *Myb*, *Gata2* and *Runx1* were downregulated in 10.5-dpc *Twist1*^{+/-} c-Kit⁺CD31⁺CD34⁺ cells,

whereas we observed upregulation of *Tal1* and no difference in *Mecom* expression (Figure 3A). We next assessed expression of *Myb*, *Gata2*, *Mecom*, *Runx1*, and *Tal1* by real-time PCR. In agreement with the IAC microarray analysis, *Myb* expression in c-Kit⁺CD31⁺CD34⁺ cells decreased in *Twist1* heterozygotes (7.69-fold, *P* = 7.4E-05) and homozygotes (250-fold, *P* = .0001) (Figure 3B) relative to WT c-Kit⁺CD31⁺CD34⁺ cells. *Gata2* expression levels in c-Kit⁺CD31⁺CD34⁺ cells also decreased in *Twist1* heterozygotes (3.86-fold, *P* = .01) and homozygotes (9.90-fold, *P* = .004) (Figure 3B) compared with that seen in WT c-Kit⁺CD31⁺CD34⁺ cells. *Runx1* expression in c-Kit⁺CD31⁺CD34⁺ cells decreased in *Twist1* heterozygotes (5.95-fold, *P* = 3.6E-05) and homozygotes (41.7-fold, *P* = 2.3E-06) (Figure 3B) relative to WT c-Kit⁺CD31⁺CD34⁺ cells. We observed no difference in *Mecom* expression in WT, *Twist1*^{+/-} and *Twist1*^{-/-} c-Kit⁺CD31⁺

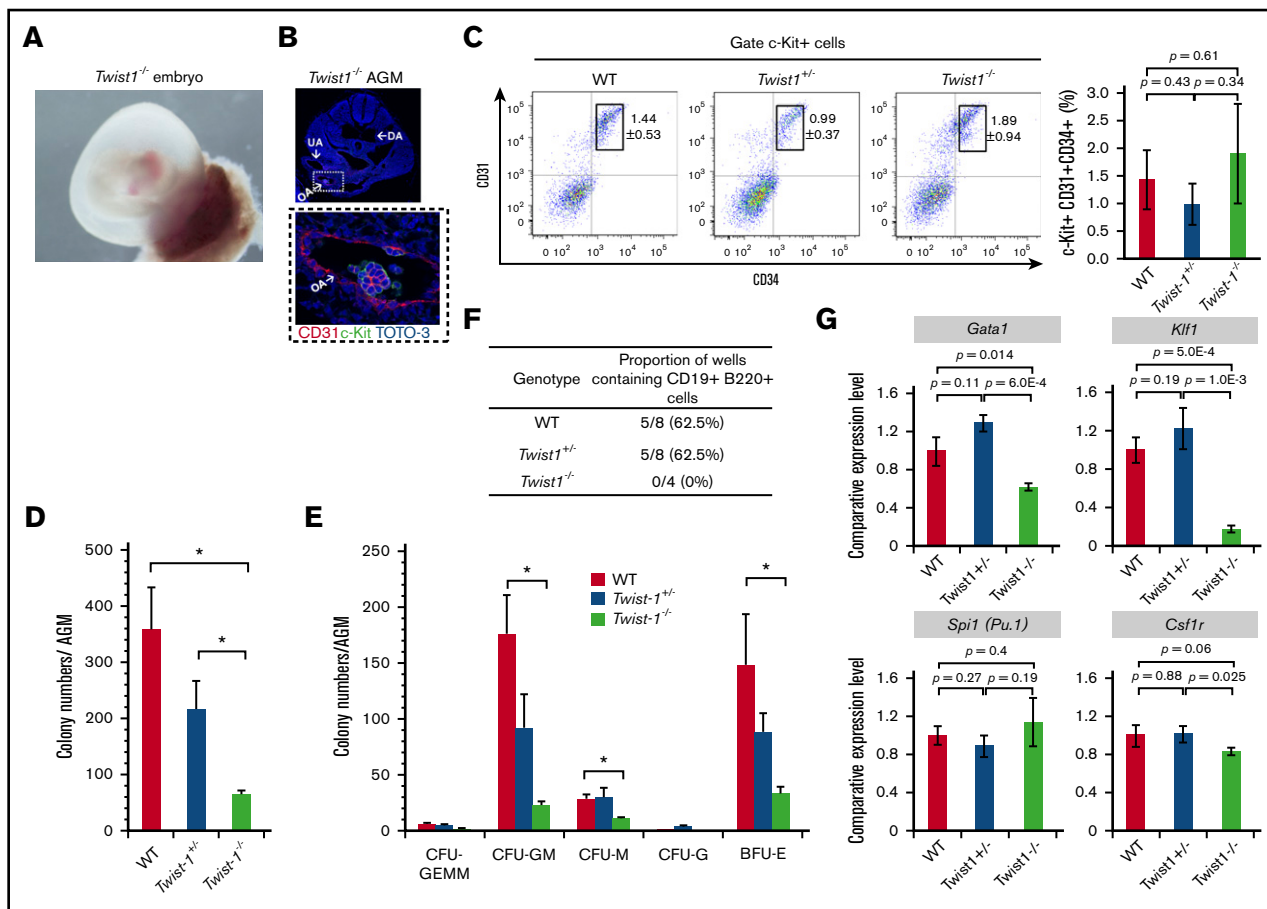


Figure 2. *Twist1*^{-/-} IACs exhibit impaired hematopoietic differentiation ability. (A) Yolk sac and placenta of *Twist1*^{-/-} mouse embryo at 10.5 dpc. (B) Immunohistochemistry of AGM tissue in *Twist1*^{-/-} embryos. Cryosections of 10.5-dpc *Twist1*^{-/-} AGM were costained with c-Kit (an HSPC marker) and CD31 (an endothelial marker) and observed by confocal microscopy. c-Kit (green), CD31 (red), and TOTO-3 iodide (blue) staining are shown. Higher magnification of OA IACs is shown in dashed box. Confocal images were acquired using a 4× (top) and 40× (bottom) objective lens. (C) Flow cytometric analysis of IACs from 10.5-dpc AGM. Bar graph shows percentage of c-Kit⁺CD31⁺CD34⁺ cells per total cells prepared from the AGM region: WT C57BL/6 mice (n = 2), *Twist1*^{+/-} mice (n = 2), and *Twist1*^{-/-} mice (n = 2). (D) HSPC CFUs. Cells were prepared from AGM from indicated genotype embryos and cultured 9 days in semisolid medium containing SCF, IL-3, IL-6, and erythropoietin (Epo). The total number of hematopoietic colonies per AGM is shown. Data shown for each genotype are from 3 embryos (n = 3). *P < .05. (E) The number of each type of hematopoietic colony in indicated genotypes. CFU-GEMM (CFU of granulocytes, erythrocytes, monocytes, and macrophages), CFU-GM (CFU of granulocytes and macrophages), CFU-M (CFU of macrophages), CFU-G (CFU of granulocytes), and BFU-E (burst-forming unit of erythroid). Data shown for each genotype are from 3 embryos (n = 3). *P < .05. (F) In vitro B lymphopoiesis assay. Single cells from AGM were cocultured 14 days with OP9 stromal cells in the presence of IL-7. CD19⁺B220⁺ cells were analyzed by flow cytometry. Percentages are defined as the number of culture wells containing CD19⁺B220⁺ cells relative to total number of culture wells. (G) Erythroid (*Gata1* and *Klf1*) and myeloid (*Spi1* and *Csf1r*) gene expression analysis of IACs prepared from the WT, *Twist1*^{+/-}, and *Twist1*^{-/-} AGM region at 10.5 dpc. Comparative expression levels were calculated using the 2^{-ΔΔCT} method. WT IAC sample served as a reference. Data shown are means ± SD of technical triplicate samples.

CD34⁺ cells. In contrast to microarray data, *Tal1* expression levels in c-Kit⁺CD31⁺CD34⁺ cells decreased in *Twist1* heterozygotes (2.07-fold, *P* = .011) and homozygotes (2.09-fold, *P* = .005) (Figure 3B) compared with that seen in WT c-Kit⁺CD31⁺CD34⁺ cells.

Overall, we conclude that *Twist1* loss impairs hematopoietic differentiation of AGM IACs, likely because of downregulation of hematopoietic transcription factor genes and, to a lesser extent, to incomplete specification of hematopoietic fate.

Twist1 binds to *Gata2* or *Myb* promoters in IACs

In *Twist1*^{-/-} IACs, the relative decrease in levels of hematopoietic transcription factor transcripts was greater than the increase in expression of endothelial genes. Thus, we investigated mechanisms underlying transcription of hematopoietic genes in c-Kit⁺CD31⁺

CD34⁺ cells. At 10.5 dpc, AGM-derived c-Kit⁺CD31⁺CD34⁺ cells expressed *Myb* and *Gata2* transcripts at levels higher than *Runx1*, *Scl* and *Mecom* transcripts (supplemental Figure 6). Thus, we focused on transcriptional regulation of *Myb* and *Gata2*. We first performed a ChIP assay by immunoprecipitating cross-linked chromatin from WT c-Kit⁺CD31⁺CD34⁺ cells with an anti-*Twist1* antibody and subjecting precipitates to PCR with primers flanking *Myb* or *Gata2* promoters (supplemental Figure 7A [*Myb*] and supplemental Figure 7B [*Gata2*], underlined). Specifically, primers were designed to amplify genomic regions flanking E-boxes “CAGTTG” in the *Myb* (supplemental Figure 7A, bold) and *Gata2* promoters (supplemental Figure 7B, bold). We observed a 0.3% of input in the case of the *Myb* promoter and a 0.0034% in the case of the *Gata2* promoter in anti-*Twist1*-precipitates derived from WT

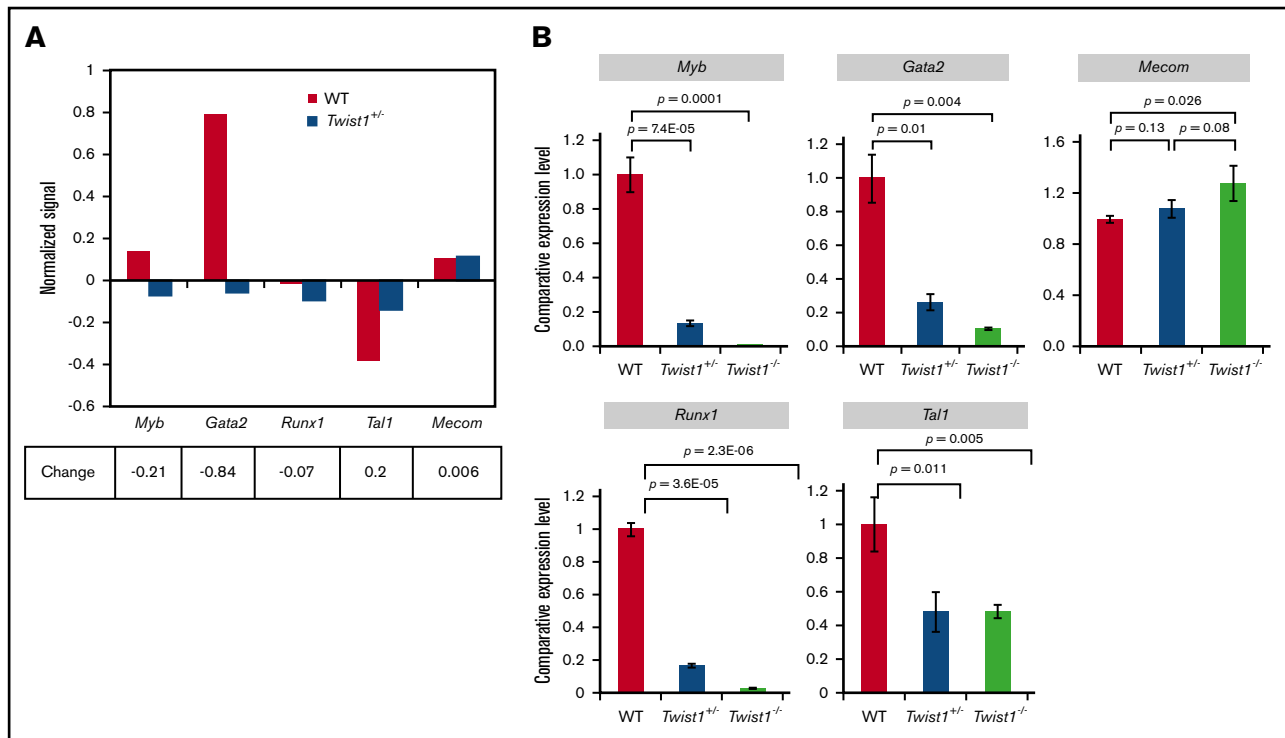


Figure 3. Gene expression analysis of hematopoietic transcription factors in 10.5-dpc IACs. (A) Gene expression analysis of WT and $Twist1^{+/-}$ IACs, as assessed by microarray. Normalized signals of indicated transcription factors are shown. Fold change was calculated by dividing the normalized signal from $Twist1^{+/-}$ IACs by the normalized signal in WT IACs. Among factors analyzed, *Myb* and *Gata2* were downregulated in $Twist1^{+/-}$ IACs. (B) Validation of microarray data. RNA from sorted c-Kit⁺CD31⁺CD34⁺ cells was extracted from 10.5-dpc AGM tissue of mice of indicated genotypes, and gene expression was assessed by real-time PCR using TaqMan probes. Comparative expression levels were calculated using the $2^{-\Delta\Delta CT}$ method. WT IAC sample served as a reference. Data shown are means \pm SD of technical triplicate samples.

CD31⁺CD34⁺c-Kit⁺ cells (Figure 4A), indicating *Twist1* enrichment on the *Myb* promoter.

We then confirmed that *Twist1* binds to the *Myb* and *Gata2* promoters by cotransfecting 293Ta cells with 2 sets of plasmids, 1 a *Twist1* expression vector and the other harboring either WT or mutated versions of *Myb* or *Gata2* promoter regions. Sequences of WT or mutant constructs were confirmed by DNA sequencing and are shown in supplemental Figure 7C-D (WT *Myb* and *Gata2* promoter [5'-CAGTTG-3']) and supplemental Figure 7E-F (mutated *Myb* and *Gata2* promoter [5'-ATGTAG-3']). When we assessed luciferase activity we observed 1.5- and 134-fold increases in luciferase activity with respective *Myb* and *Gata2* promoters, relative to control empty *Twist1* expression vector (see Mock-*Myb* or Mock-*Gata2* promoter in Figure 4B-C). *Twist1* binding specificity was confirmed by comparable cotransfections using plasmids harboring mutant promoters: luciferase activity was significantly decreased by 0.18-fold ($P = 3.3E-06$) and 0.37-fold ($P = .00048$) in respective cotransfections with mutant *Myb* (Figure 4B, *Twist*-Mutant *Myb* promoter) or *Gata2* promoter (*Twist*-mutant *Gata2* promoter) plasmids. These results strongly suggest that *Twist1* directly binds to *Myb* and *Gata2* promoters in c-Kit⁺CD31⁺CD34⁺ IACs of the 10.5-dpc AGM region.

Discussion

Here we demonstrate that *Twist1* is highly expressed in embryonic HSPCs in the AGM region and functions as a hematopoietic

transcription factor in HSPC differentiation through binding to *Myb* and *Gata2* promoter regions.

High *Twist* expression in AGM-derived HSPCs relative to that in FL- and BM-derived HSPCs suggests the importance of *Twist1* in hematopoietic development and/or differentiation (Figure 1B). Our in vitro differentiation assay showing that *Twist1* loss impairs differentiation of AGM-derived HSPCs (Figure 2E) confirms this hypothesis. Moreover, expression of *Myb* and *Gata2* messenger RNA is severely suppressed in *Twist1* knockout AGM-derived HSPCs (Figure 3A-B); that finding combined with our ChIP analysis of the *Myb* and *Gata2* promoters strongly suggests that *Twist1* directly regulates transcription of *Myb* and *Gata2* genes.

In agreement with the normal hematopoiesis seen in adult $Twist1^{+/-}$ mice, $Twist1^{+/-}$ AGM- and FL-derived HSPCs possess unimpaired differentiation ability, findings in contrast with *Runx1* haploinsufficiency phenotypes: heterozygous *Runx1* mice show lethality and severely impaired embryonic hematopoiesis by midgestation.¹² However, *Twist1* heterozygous embryos do not display impaired hematopoiesis, implying that a single functional copy of *Twist1* is sufficient for hematopoietic differentiation.

Twist1 reportedly functions in HSPC differentiation: *Twist1* overexpression activates expression of *Gata1* and *Spi1* (*Pu.1*) transcripts in adult BM-derived HSPCs, skewing HSPC differentiation toward the myeloid lineage.³³ In agreement, we found that *Twist1* loss suppressed *Gata1* expression in AGM-derived HSPCs,

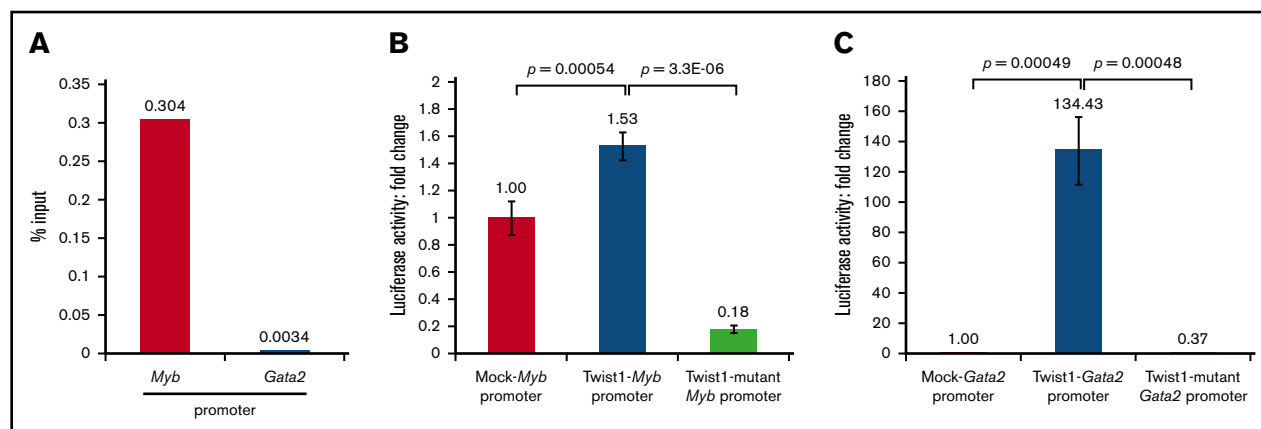


Figure 4. Transcriptional regulation by Twist1 in 10.5-dpc IACs. (A) ChIP was performed in c-Kit⁺CD31⁺CD34⁺ cells from 10.5-dpc AGM of WT mice, and real-time PCR was employed to amplify promoter regions of *Myb* or *Gata2*. (B) *Myb* promoter activation by Twist1. 293T cells were cotransfected with *Myb* promoter- and mutant *Myb* promoter-containing luciferase plasmids plus a *Twist1* expression plasmid, and luciferase activity was analyzed as fold change, calculated as the signal of Twist-*Myb* or Twist-mutant *Myb* promoters divided by the signal from the mock (promoterless)-*Myb* vector (set to “1” in the bar graph). Fold changes and error bars are respective means and SDs calculated from triplicate wells. (C) *Gata2* promoter activation by Twist1. Shown are analyses comparable to those in panel B.

impairing myeloid differentiation (Figure 2E,G). However, we observed no change in expression of the myeloid transcription factor *Spi1* (*Pu.1*) in *Twist1*^{-/-} embryos. This discrepancy may be because of the fact that diverse mechanisms regulate differentiation of adult and embryonic HSPCs, a hypothesis based on a previous report that *Gata2* plays functionally distinct roles in AGM and adult BM HSPCs.³⁴

Twist1 is a transcriptional regulator that binds to a CANNTG hexanucleotide sequence, a motif known as an E-box.^{21,22} We report that *Twist1* is seen in the nucleus of IACs (Figure 1C). Furthermore, we have identified a CAGTTG E-box at the 5'-end of *Myb* and *Gata2* transcriptional start sites, where promoters are located, and designed primers for ChIP to amplify sequences containing those E-boxes. Consistent with previous reports,^{21,22} our ChIP and luciferase analysis confirmed *Twist1* binding to CAGTTG (Figure 4B-C).

ChIP analysis revealed that *Twist1* protein was more enriched on the *Myb* than on the *Gata2* promoter in AGM-derived IACs, but a luciferase reporter assay undertaken in 293T cells showed more robust transcriptional activity by *Twist1* protein on the *Gata2* compared with the *Myb* promoter in 293T cells. ChIP analysis indicates the extent of protein binding to DNA *in vivo*; by contrast, our luciferase assay directly assessed *Twist1* transcriptional activity in transfected 293T cells, in a cell and chromatin context likely different from AGM-derived IACs. Taken together, these data suggest that the readout of each ChIP and luciferase assays cannot be compared quantitatively.

Since expression of *Myb* and *Gata2* in WT IAC was higher than that of *Runx1* and *Tal1* (supplemental Figure 7), we focused on transcriptional regulation of *Myb* and *Gata2*. *Gata2* is reportedly essential for differentiation of hematopoietic precursors³⁵ and for the ETH cell transition¹⁴ in mouse embryos. Although *Mecom* has been recently implicated in embryonic HSPC generation by regulating that transition,¹⁶ we did not observe changes in levels of *Mecom* transcripts in *Twist1*^{-/-} embryos (Figure 3B), suggesting that impairment of the ETH transition is likely because of

downregulated *Gata2* gene expression. *Myb*, also known as c-*Myb*, is required for HSPC differentiation in mouse embryos and adults. *Myb*^{-/-} embryos exhibit severe anemia from 14 dpc onward.¹³ Impairment of multilineage hematopoietic progenitor cells in *Myb*^{-/-} adult mice has also been reported.³² In agreement, we also observed impaired hematopoietic differentiation of *Twist1*^{-/-} IACs. Thus, we propose that *Twist1* regulates IAC differentiation by binding to respective *Gata2* and *Myb* promoters.

To our knowledge, it is not known whether *Twist1* protein interacts with *Gata2* or *Myb* protein or *Gata2* protein interacts with *Myb* protein. To address these questions, we performed protein-protein interaction analysis using STRING (Search Tool for the Retrieval of Interacting Genes/Proteins).³⁶ As shown in supplemental Figure 8, we observed no *Twist1*-*Gata2*, *Twist1*-*Myb*, or *Gata2*-*Myb* interactions, implying that *Twist1* protein regulates *Gata2* and *Myb* at the transcriptional level and that *Gata2* and *Myb* independently regulate differentiation.

Key hematopoietic transcription factors functioning in HSPC development² are reportedly important for leukemogenesis: MYB is required for B-cell leukemogenesis³⁷ and GATA2 overexpression is observed in acute myeloid leukemia.³⁸ However, a function for *Twist1* in either HSPC development or leukemogenesis has been largely unknown. In this study, high levels of *Twist1* transcripts were observed in embryonic relative to adult HSPCs (Figure 1B), suggesting that *Twist1* functions in embryonic hematopoiesis. Likewise, differentiation of *Twist1*^{-/-} embryonic HSPCs into myeloid and B lymphoid lineages was impaired, implying a potential role for *Twist1* in pathways common to hematopoietic development and leukemogenesis (Figure 2E-F). Further investigation of TWIST1 in human hematopoiesis should provide additional insight into mechanisms governing normal and abnormal hematopoiesis.

Acknowledgments

The authors thank Keai Sinn Tan, Yuka Tanaka, and Ayako Takai for technical support, and Elise Lamar for critical reading of the manuscript.

This work was supported by the Ministry of Education, Culture, Sports, Science and Technology; the Ministry of Health, Labor and Welfare; and the Japan Society for the Promotion of Science.

Authorship

Contribution: K.K. and T. Inoue performed experiments, analyzed data, and wrote the manuscript; T. Iino performed experiments; K.T. and K.A. advised on the study; N.A.S. provided Twist1 mutant mice and advice; Y.N. provided advice on the study; and D.S. designed the

study, performed experiments, analyzed and interpreted data, and wrote the manuscript.

Conflict-of-interest disclosure: The authors declare no competing financial interests.

Correspondence: Daisuke Sugiyama, Department of Research and Development of Next Generation Medicine, Faculty of Medical Sciences, Kyushu University, Station for Collaborative Research 1, 4F, 3-1-1 Maidashi, Higashi-Ku, Fukuoka 812-8582, Japan; e-mail: ds-mons@yb3.so-net.ne.jp.

References

1. Dieterlen-Lièvre F, Pouget C, Bollérot K, Jaffredo T. Are intra-aortic hemopoietic cells derived from endothelial cells during ontogeny? *Trends Cardiovasc Med*. 2006;16(4):128-139.
2. Dzierzak E, Speck NA. Of lineage and legacy: the development of mammalian hematopoietic stem cells. *Nat Immunol*. 2008;9(2):129-136.
3. Godin I, Cumano A. The hare and the tortoise: an embryonic haematopoietic race. *Nat Rev Immunol*. 2002;2(8):593-604.
4. Jaffredo T, Bollérot K, Sugiyama D, Gautier R, Drevon C. Tracing the hemangioblast during embryogenesis: developmental relationships between endothelial and hematopoietic cells. *Int J Dev Biol*. 2005;49(2-3):269-277.
5. Mikkola HK, Orkin SH. The journey of developing hematopoietic stem cells. *Development*. 2006;133(19):3733-3744.
6. Sugiyama D, Tsuji K. Definitive hematopoiesis from endothelial cells in the mouse embryo; a simple guide. *Trends Cardiovasc Med*. 2006;16(2):45-49.
7. Taoudi S, Gonneau C, Moore K, et al. Extensive hematopoietic stem cell generation in the AGM region via maturation of VE-cadherin+CD45+ pre-definitive HSCs. *Cell Stem Cell*. 2008;3(1):99-108.
8. Garcia-Porrero JA, Godin IE, Dieterlen-Lièvre F. Potential intraembryonic hemogenic sites at pre-liver stages in the mouse. *Anat Embryol (Berl)*. 1995;192(5):425-435.
9. Garcia-Porrero JA, Manaia A, Jimeno J, Lasky LL, Dieterlen-Lièvre F, Godin IE. Antigenic profiles of endothelial and hemopoietic lineages in murine intraembryonic hemogenic sites. *Dev Comp Immunol*. 1998;22(3):303-319.
10. Mizuochi C, Fraser ST, Biasch K, et al. Intra-aortic clusters undergo endothelial to hematopoietic phenotypic transition during early embryogenesis. *PLoS One*. 2012;7(4):e35763.
11. North T, Gu TL, Stacy T, et al. Cbfa2 is required for the formation of intra-aortic hematopoietic clusters. *Development*. 1999;126(11):2563-2575.
12. Cai Z, de Bruijn M, Ma X, et al. Haploinsufficiency of AML1 affects the temporal and spatial generation of hematopoietic stem cells in the mouse embryo. *Immunity*. 2000;13(4):423-431.
13. Mucenski ML, McLain K, Kier AB, et al. A functional c-myc gene is required for normal murine fetal hepatic hematopoiesis. *Cell*. 1991;65(4):677-689.
14. de Pater E, Kaimakis P, Vink CS, et al. Gata2 is required for HSC generation and survival. *J Exp Med*. 2013;210(13):2843-2850.
15. Pimanda JE, Donaldson IJ, de Bruijn MF, et al. The SCL transcriptional network and BMP signaling pathway interact to regulate RUNX1 activity. *Proc Natl Acad Sci USA*. 2007;104(3):840-845.
16. Konantz M, Alghisi E, Müller JS, et al. Evi1 regulates Notch activation to induce zebrafish hematopoietic stem cell emergence. *EMBO J*. 2016;35(21):2315-2331.
17. Goyama S, Yamamoto G, Shimabe M, et al. Evi-1 is a critical regulator for hematopoietic stem cells and transformed leukemic cells. *Cell Stem Cell*. 2008;3(2):207-220.
18. Sugiyama D, Joshi A, Kulkeaw K, et al. A transcriptional switch point during hematopoietic stem and progenitor cell ontogeny. *Stem Cells Dev*. 2017;26(5):314-327.
19. Sasaki T, Tanaka Y, Kulkeaw K, et al. Embryonic intra-aortic clusters undergo myeloid differentiation mediated by mesonephros-derived CSF1 in mouse. *Stem Cell Rev*. 2016;12(5):530-542.
20. Bialek P, Kern B, Yang X, et al. A twist code determines the onset of osteoblast differentiation. *Dev Cell*. 2004;6(3):423-435.
21. Connerney J, Andreeva V, Leshem Y, Muentener C, Mercado MA, Spicer DB. Twist1 dimer selection regulates cranial suture patterning and fusion. *Dev Dyn*. 2006;235(5):1334-1346.
22. Firulli BA, Krawchuk D, Centonze VE, et al. Altered Twist1 and Hand2 dimerization is associated with Saethre-Chotzen syndrome and limb abnormalities. *Nat Genet*. 2005;37(4):373-381.
23. Livak KJ, Schmittgen TD. Analysis of relative gene expression data using real-time quantitative PCR and the 2⁻(Delta Delta C(T)) method. *Methods*. 2001;25(4):402-408.
24. Bildsoe H, Loebel DAF, Jones VJ, Chen YT, Behringer RR, Tam PPL. Requirement for Twist1 in frontonasal and skull vault development in the mouse embryo. *Dev Biol*. 2009;331(2):176-188.
25. Chen ZF, Behringer RR. twist is required in head mesenchyme for cranial neural tube morphogenesis. *Genes Dev*. 1995;9(6):686-699.

26. Kaufman MH. The Atlas of Mouse Development. London, United Kingdom: Elsevier Academic Press; 1992.
27. Sugiyama D, Ogawa M, Nakao K, et al. B cell potential can be obtained from pre-circulatory yolk sac, but with low frequency. *Dev Biol.* 2007;301(1):53-61.
28. Rao X, Huang X, Zhou Z, Lin X. An improvement of the 2⁻(-delta delta CT) method for quantitative real-time polymerase chain reaction data analysis. *Biostat Bioinforma Biomath.* 2013;3(3):71-85.
29. Suzuki A, Wakaguri H, Yamashita R, et al. DBTSS as an integrative platform for transcriptome, epigenome and genome sequence variation data. *Nucleic Acids Res.* 2015;43(D1):D87-D91.
30. Solaimani Kartalaei P, Yamada-Inagawa T, Vink CS, et al. Whole-transcriptome analysis of endothelial to hematopoietic stem cell transition reveals a requirement for Gpr56 in HSC generation. *J Exp Med.* 2015;212(1):93-106.
31. Swiers G, Baumann C, O'Rourke J, et al. Early dynamic fate changes in haemogenic endothelium characterized at the single-cell level. *Nat Commun.* 2013;4:2924.
32. Sandberg ML, Sutton SE, Pletcher MT, et al. c-Myb and p300 regulate hematopoietic stem cell proliferation and differentiation. *Dev Cell.* 2005;8(2):153-166.
33. Dong CY, Liu XY, Wang N, et al. Twist-1, a novel regulator of hematopoietic stem cell self-renewal and myeloid lineage development. *Stem Cells.* 2014;32(12):3173-3182.
34. Ling KW, Ottersbach K, van Hamburg JP, et al. GATA-2 plays two functionally distinct roles during the ontogeny of hematopoietic stem cells. *J Exp Med.* 2004;200(7):871-882.
35. Minegishi N, Suzuki N, Yokomizo T, et al. Expression and domain-specific function of GATA-2 during differentiation of the hematopoietic precursor cells in midgestation mouse embryos. *Blood.* 2003;102(3):896-905.
36. Szklarczyk D, Morris JH, Cook H, et al. The STRING database in 2017: quality-controlled protein-protein association networks, made broadly accessible. *Nucleic Acids Res.* 2017;45(D1):D362-D368.
37. Waldron T, De Dominicis M, Soliera AR, et al. c-Myb and its target Bmi1 are required for p190BCR/ABL leukemogenesis in mouse and human cells. *Leukemia.* 2012;26(4):644-653.
38. Vicente C, Vazquez I, Conchillo A, et al. Overexpression of GATA2 predicts an adverse prognosis for patients with acute myeloid leukemia and it is associated with distinct molecular abnormalities. *Leukemia.* 2012;26(3):550-554.